Journal of Molecular Structure 1038 (2013) 177–187

Contents lists available at SciVerse ScienceDirect

Journal of Molecular Structure

journal homepage: www.elsevier.com/locate/molstruc

Theoretical and spectroscopic studies on molecular structure and hydrogen bonding of 1,2-bis (monochloroacetyl) cyclopentadiene

Sayyed Faramarz Tayyari [a,*], Somayeh Laleh [b], Mansoureh Zahedi-Tabrizi [c], Mohammad Vakili [b]

[a] Chemistry Department, Shahrood Branch, Islamic Azad University, Shahrood, Iran
[b] Chemistry Department, Ferdowsi University of Mashhad, Mashhad 91775-1436, Iran
[c] Chemistry Department, Alzahra University, Tehran, Iran

HIGHLIGHTS

- 1,2-Bis (monochloroacetyl) cyclopentadiene forms a short-strong H-bond.
- Formation of hydrogen bond is confirmed by experimental and theoretical methods.
- The H-bond is assisted by π-electron delocalization through the CP ring.
- The potential energy barrier for proton transfer in MCACP is low.
- The scaled theoretical frequencies are in good agreement with the experimental data.

ARTICLE INFO

Article history:
Received 9 November 2012
Received in revised form 10 January 2013
Accepted 12 January 2013
Available online 1 February 2013

Keywords:
Strong hydrogen bond
Vibrational spectra
Density functional theory
1,2-Bis (monochloroacetyl) cyclopentadiene
Rotation barriers
Intramolecular hydrogen bond

ABSTRACT

1,2-Bis (monochloroacetyl) cyclopentadiene (MCACP) was synthesized and its molecular structure, intramolecular hydrogen bonding, and vibrational frequencies were investigated by means of density functional theory (DFT) calculations, NMR, and IR spectroscopies. It was found that the most stable conformers are those stabilized by intramolecular hydrogen bridges. Calculations at the B3LYP level, using 6-31G(d,p), 6-311G(d,p), and 6-311++G(d,p) basis sets, have been carried out for understanding the strength of hydrogen bond. In addition, the energies of the stable chelated conformers and their corresponding open structures were obtained at the MP2/6-31G(d,p) level of theory. The harmonic vibrational wavenumbers of MCACP and its deuterated analogue were obtained at the B3LYP/6-311++G(d,p) level. ^{1}H and ^{13}CNMR spectra were recorded and ^{1}H and ^{13}C nuclear magnetic resonance chemical shifts of the molecule were calculated using the gauge independent atomic orbital (GIAO) method. The calculated geometrical parameters and relative energies show formation of a very strong intramolecular hydrogen bond that is consistent with the frequency shifts for OH/OD stretching, OH/OD out-of-plane bending, and O···O stretching modes and proton chemical shift. The rotation of terminal CH_2Cl groups indicates existence of two stable conformers that their hydrogen bond energy was estimated to be, on average, about 75.6 kJ/mol. The nucleus-independent chemical shift (NICS) data in the keto and enol forms indicated that in addition to differences in stability due to hydrogen bonding, differing stability also arises from the aromaticity increase of cyclopentadene (CP) ring in the chelated forms.

1. Introduction

It is well known that the intramolecular hydrogen bond has an interesting effect on the physicochemical properties and its role was extensively studied as a structural organizing feature in chemistry [1–4]. Over many years, a large group of β-diketones that are important organic reagents have been of great interest to organic, inorganic, bio, and physical chemistry. These compounds are often investigated both experimentally and by theoretical methods [5–8]. It is well known that the strength of the hydrogen bond depends on the electronegativity of the atoms attached to the hydrogen atom, atomic charges, conjugation of the chelated ring, and etc. Charge assisted hydrogen bonding (CAHB) and resonance assisted hydrogen bonding (RAHB) are the two important factors for strengthening of hydrogen bond in such systems which was introduced by Gilli et al. [9]. In these systems, three geometrical characterizations could be considered: (i) the equalization of C—O and C=O (ii) and the C=C and C=C bond lengths, and (iii) the elongation of the O—H bond, and shortening of the O···O distance.

* Corresponding author. Tel.: +98 511 8780216; fax: +98 511 8438032.
E-mail address: Tayyari@ferdowsi.um.ac.ir (S.F. Tayyari).

0022-2860/$ - see front matter © 2013 Elsevier B.V. All rights reserved.
http://dx.doi.org/10.1016/j.molstruc.2013.01.031

The hydrogen bonding energy (E_{HB}) of the intramolecular hydrogen bonded systems cannot be measured experimentally and its magnitude could be estimated only with theoretical calculations. E_{HB} is a relative energy (E_R) between energy of hydrogen-bonded structure (chelated form) and that of non-hydrogen bonded structure (open form).

Recently, special attention has been focused on short-strong hydrogen bonds (SSHBs) with low barriers to proton transfer, so-called low-barrier H-bonds (LBHBs). These systems which can stabilize transition states in enzyme catalyzed biochemical pathways [10–13], are characterized by their large hydrogen bond energies (>42 kJ/mol), short O···O distances (<2.6 Å), and large downfield shift of NMR resonances (>15 ppm) [14,15]. Two factors were identified as being important for formation of strong hydrogen bonds, steric and electronic factors [16,17].

1,2 Diacylcyclopentadienes categorized to the SSHB class of compounds. In the enol form of these compounds because of intramolecular hydrogen bond formation and a long π-electronic conjugation between carbonyl and CP double bonds, a heptagonal (see Fig. 1) is formed which is referred to as a chelated ring. Since this seven-membered ring is larger than six-membered ring of β-dicarbonyls, spatial coordinates are more proper to form much stronger hydrogen bond (O—H···O) in 1,2 diacylcyclopentadienes than that in the enol forms of β-dicarbonyls. In spite of extensive works on structure and properties of intramolecular hydrogen bonds in the enol forms of β-dicarbonyl compounds, only a few reports are appeared in the literatures about the hydrogen bonding nature in 1,2 diacylcyclopentadienes. These compounds solely exist in the enol form and their proton chemical shifts are consistent with a very strong hydrogen bond [18–20]. Diformylcyclopentadiene (DFCP) and diacetylcyclopentadiene (DACP) are the simplest members of diacylcyclopentadiene group, which was named ζ-dicarbonyl by Gilli and Bertolasi [21]. Diacylcyclopentadiene compounds are potentially capable of forming complexes with metal ions [22] and are interesting compounds for study of hydrogen bond nature. MCACP is a member of diacylcyclopentadiene compounds.

The aim of the present paper is study of conformational analysis, hydrogen bond energy, barrier to rotation energy of the CH_2Cl groups, proton tunneling barrier height, vibrational frequencies, and solvent effect on the conformation stability and the strength of the intramolecular hydrogen bond. The obtained results are compared with the corresponding results for the most stable conformer of 1,2-bis (dichloroacetyl) cyclopentadiene (DCACP) [23] and some β-diketones.

2. Computational methods

In this study, the calculations for molecular equilibrium geometry and vibrational spectra of MCACP were performed by means of the Gaussian 09W software package [24]. All possible tautomers and conformers were fully optimized at the B3LYP level [25,26], using 6-31G(d,p), 6-311G(d,p), and 6-311++G(d,p) basis sets. The stability energies of the chelated enols and their corresponding open structures were also fully optimized at the MP2/6-31G(d,p) level. Vibrational frequencies of both stable chelated conformers of MCACP and their partially deuterated analogues, D-MCACP, were calculated at the B3LYP level using 6-311++G(d,p) basis set in the gas phase and carbontetrachloride solution.

The assignment of the experimental frequencies are based on the observed band frequencies and intensity changes in the infrared spectra of the deuterated species and confirmed by establishing one to one correlation between observed and theoretically calculated frequencies. The assignment of the calculated wavenumbers was aided by the animation option of the GaussView 5.0 graphical interface for Gaussian programs [27], which gives a visual representation of the shape of the vibrational modes.

The solvent effect and its interaction with MCACP molecule were studied by using Polarizable Continuum Model (PCM) [28–30] in which the cavity is created via a series of overlapping spheres. The geometry, stability energy, and hydrogen bonding energy of MCACP conformers were obtained at the B3LYP level, using 6-311G(d,p) and 6-311++G(d,p) basis sets, with media relative permittivities of $CHCl_3$ and CH_3COCH_3.

^1H and ^{13}C NMR chemical shifts are calculated within GIAO approach [31,32] applying B3LYP method with 6-311++G(d,p) basis set. The theoretical NMR ^1H and ^{13}C chemical shift values were obtained by subtracting the GIAO calculated ^1H and ^{13}C isotropic magnetic shielding (σ) of any hydrogen or carbon atom from the average ^1H or ^{13}C isotropic magnetic shielding of TMS (σ_0), respectively ($\delta = \sigma_0 - \sigma$).

In the NICS study [33], the gauge invariant atomic orbital (GIAO) method was applied on the B3LYP/6-311++G(d,p) optimized structures to estimate the magnetic shielding tensor.

Bond orders were obtained by Natural Bond Orbital (NBO) program [34]. NBO analysis for all chelated and open structures were calculated at the B3LYP level using 6-311++G(d,p) basis set.

To explore the proton tunneling, the OH distance was varied from 0.9 to 1.24 Å and the OOH angle was varied from 0° to 25° and calculated the energies at the B3LYP/6-311++G(d,p) level by

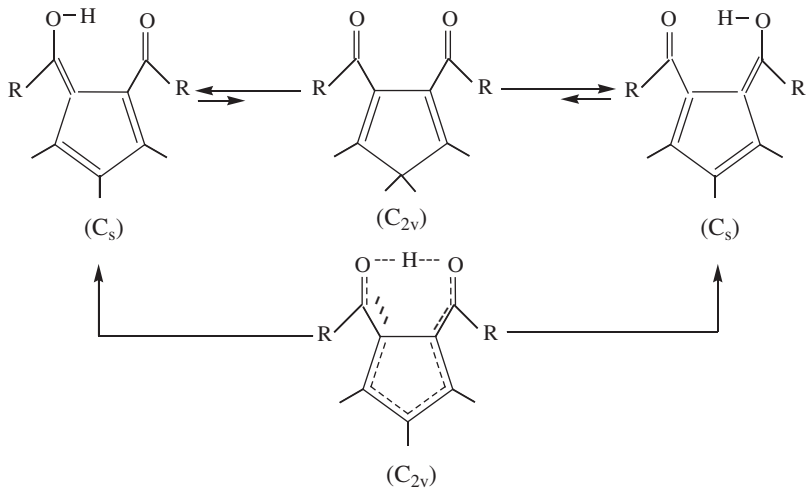

Fig. 1. The keto-enol tautomerization in 1,2 diacylcyclopentadienes.

keeping all other structural parameters at their optimized equilibrium positions. The potential energy surfaces obtained at this level were fitted to the following anharmonic two dimensional potential function:

$$2V = K_s X^2 + K_{ss} X^4 + K_b Y^2 + K_{ssb} X^2 Y \quad (1)$$

using Genplot package for three-dimensional non-linear fit [35], where K_s and K_{ss} represent the quadratic and quartic force constants in the X (stretching) direction, respectively, K_b represents the quadratic force constant in the Y (bending) direction and K_{ssb} represent the interaction between stretching and bending modes. Inclusion of other terms such as X^6, Y^3 and cross-terms such as X^2Y^2 and X^2Y^3 did not improve the fitting and thus were not used.

The calculations for determining the CH_2Cl barrier to rotation were carried out separately on each of the two monochloro methyl groups; next the same calculations were performed by considering a synchronous rotation of both CH_2Cl groups. The energy was calculated at 15° steps in the monochloro methyl group rotation (at the 6-311++G(d,p) level), while all other geometrical parameters were relaxed to be fully optimized.

3. Experimental

3.1. Material

The MCACP synthesis essentially follows the method of Linn and Sharkey [36], which reported a method for the benzoylation of cyclopentadienyllithium. MCACP was prepared from cyclopentadienyllithium which obtained from phenyllithium and freshly distilled CP. Then, to this solution dilute monochloroacetyl chloride was added dropwise in argon atmosphere. The reaction mixture was hydrolyzed with dilute acetic acid and organic layer separated and this procedure was repeated three times. The extracted layers were dried over Na_2SO_4 and solvent was removed to form yellow crystal solid.

The partially deuterated MCACP (D-MCACP), was prepared by mixing the CCl_4 solution of MCACP with D_2O. Then the organic layer was separated and dried over Na_2SO_4. This method was repeated twice. The synthesized compound and its deuterated analogue were investigated by IR, ^{1}HNMR, and ^{13}CNMR spectroscopy methods.

3.2. Equipment

All Mid-IR spectra were obtained with a Bomem MB-154 Fourier Transform Spectrophotometer. The solid and solution spectra were measured as KBr disc and CCl_4 solution in the range of 4000–500 cm^{-1} with resolution of 2 cm^{-1} by averaging the results of 25 scans.

Because of strong fluorescence background, all attempts for obtaining an acceptable Raman spectrum of MCACP were unsuccessful.

The Far-IR spectra were recorded using a Thermo Nicolet NEXUS 870 FT-IR spectrometer equipped with a DTGS/polyethylene detector and a solid substrate beam splitter. The spectrum of this region that consists of 600–250 cm^{-1} was collected with a resolution of 2 cm^{-1} by signal averaging the results of 64 scans.

The NMR spectra were obtained on solutions in $CDCl_3$. The results were obtained on a FT-NMR, Brucker DRX 500 AVANCE spectrometer equipped with a z-gradient accessory and an inverse (or direct detection) 5 mm diameter probehead working at 500.13 MHz for ^{1}H and 125.76 MHz for ^{13}C. The chemical shifts were referenced to the signal of TMS.

4. Results and discussion

4.1. Conformation analysis and tautomerism

According to the theoretical calculations, among the probable conformers of MCACP only two of them are engaged in a seven-member chelated ring to form an intramolecular hydrogen bond (labeled as A-I and A-II in Fig. 2). These two possible chelated conformers are distinguished by relative position of both CH_2Cl groups. The repulsion between two chlorine atoms in A-II conformer makes it slightly more unstable than A-I conformer.

In addition to the enol tautomers, six diketo tautomers can also be considered for MCACP, which are shown in Fig. 3. For comparison, the relative energies of all tautomers and conformers of MCACP are calculated at the B3LYP/6-311++G(d,p) level and are given in Figs. 2 and 3. Our calculations in the gas phase indicate that the keto forms are 56.1–72.5 kJ/mol less stable than the most stable chelated form. Therefore, coexisting of any keto form in the sample is unlikely. Such high relative stability can be attributed to the intramolecular hydrogen bond formation that is absent in the keto (C) and open enol conformers (B).

Another factor that can be effective on relative stability of chelated forms is the CP aromaticity. To determine the aromaticity changes of the CP ring in the enol and keto structures of MCACP, (NICS) values were calculated at above CP ring from 0.0 to 4.5 Å with a step size of 0.5 Å. Fig. 4 shows the change in aromaticity of CP ring in the chelated forms and their corresponding open structures. To study of the CP ring aromaticity, the most stable keto structure (C-II) was considered. It is noteworthy that the CP ring in the enol and keto forms is aromatic. As it is shown in Fig. 4 the aromaticity increases according to the following trend:

$$A-I > A-II > C-II > B-II > B-I$$

This trend is consistent with the relative stability energies. Two factors are responsible for high degree of aromaticity in the CP ring of the cis-enol forms. The first factor is formation of the strong intramolecular hydrogen bond, which assist the π-electron conjugation in the CP ring. The second factor is the coplanarity of the chelated and CP rings. In the trans-enol forms (open structures) intramolecular hydrogen bond is absent and the C═O bond is no longer coplanar with the CP ring. The aromaticity of the keto form, which one of its C═O bonds is in the plane of the CP ring, is slightly higher than that of the trans-enol forms. This result suggests that the intramolecular hydrogen bond plays an important role in increasing the aromaticity in CP ring.

4.2. Geometrical parameters of the enol forms

The geometries of open and chelated enol forms of MCACP along with the numbering of the atoms are given in Fig. 2. The geometry of the possible keto forms are illustrated in Fig. 3. Some of the most important geometrical parameters of the full optimized chelated and open structures along with the geometry of fulvene, for comparison, are collected in Table 1. The most important parameter which is related to the hydrogen bond strength in this molecule is O7···O9 distance. Calculations at the B3LYP/6-311++G(d,p) level in the gas phase predict an O7···O9 distance of about 2.490 Å for both A-I and A-II conformers. The corresponding value in the most stable conformer of DCACP is 2.472 Å [23]. This result indicates that substitution of additional Cl atoms increases the hydrogen bond strength. It seems that the columbic repulsive and steric effects between the Cl and O atoms in DCACP are more important than its electron withdrawing effect. The position of the Cl atoms in DCACP, therefore their steric effect, has compensated their electron withdrawing effect. The final result of these

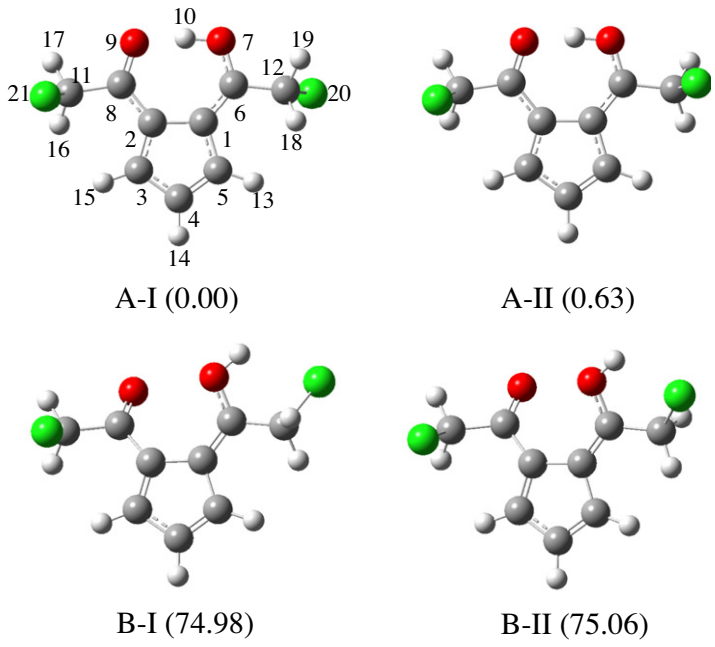

Fig. 2. Atom numbering and possible stable chelated (A) and open (B) enol conformers of MCACP calculated at the B3LYP/6-311++G(d,p) level. The relative energies (kJ/mol) are given in parentheses.

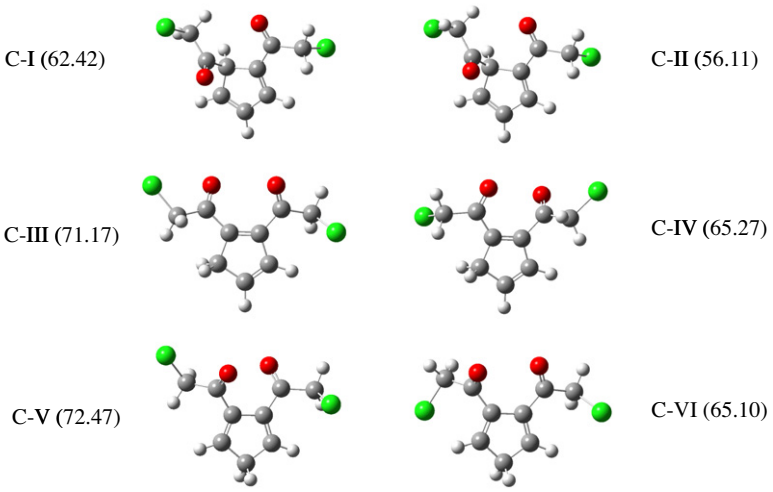

Fig. 3. Possible keto tautomers of MCACP and their relative energies (kJ/mol) compared with the most stable enol form.

two opposite effects was further reduction of the O7···O9 distance in DCACP compared with that for MCACP. The calculated results indicate that the O7···O9 distance in MCACP (about 2.490 Å) is considerably shorter than the corresponding value for β-diketones such as malonaldehyde (MA) (2.587 Å [37]), acetylacetone (AA) (2.544 Å [38]), and hexafluoro-acetylacetone (HFAA) (2.592 Å [39]). It is noteworthy that the hydrogen bond in this system is very near to linear (the O7H10O9 bond angle is about 170.5°), while the hydrogen bond in the enol forms of β-diketones is considerably deviates from linearity. This linearity, in addition to the shortening of O7···O9 distance, makes the hydrogen bond in these system very strong, which is in agreement with the NMR results. Also, solid state X-ray and neutron diffraction data for 6-hydroxy-1-formylfulvene (HFF) show that the O···O distance is about 2.513 Å [18]. For two other members of diacylcyclopentadiene derivatives, 2,3-diacetyl-5-nitrocyclopentadiene and 2,3-dibenzoyl-5-nitrocyclopentadiene [40], the reported O···O distance is 2.446 and 2.433 Å, respectively.

The calculated results (Table 1) indicate that the C8—C11 and C6—C12 bond lengths in MCACP are 1.521 and 1.504 Å, respectively, which are longer than the analogous values for C—CH_3 bond length in AA, 1.511 and 1.494 Å [41]. The corresponding calculated values for DCACP are 1.534 and 1.514 Å [23]. To explain this behavior two effects could be considered. (1) The electrostatic effects of substituted groups [39]. (2) The nCl to σ^*C—C electron delocalization. On the other hand, the calculated O7-H10 bond length in both stable chelated conformers of MCACP is 1.035 Å, which is 0.004 Å shorter than that in the most stable DCACP conformer [23].

According to the calculated results (Table 1), the C=C and C—C bond lengths in the CP ring of the title compound is longer and

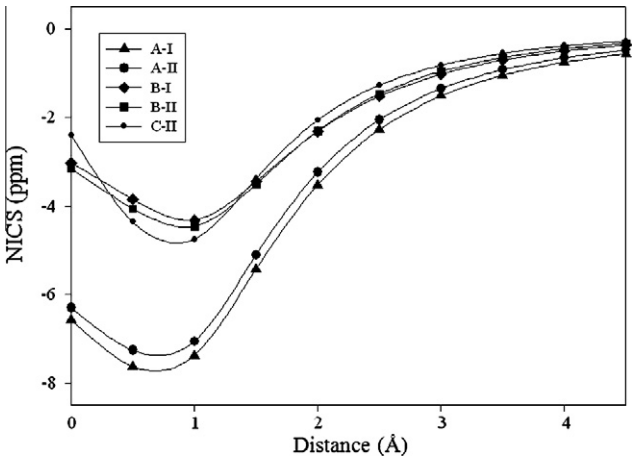

Fig. 4. Plot of the calculated NICS values (ppm) vs distance (Å) from 0.0 to 4.5 Å above the CP ring in the enol and keto forms.

shorter than the corresponding values in fulvene molecule, respectively. These differences reveal that in MCACP molecule, the intramolecular hydrogen bond is assisted by the π-electron delocalization through the CP ring. Calculations also show that the C1—C2 bond length difference in open and chelated structures is insignificant which suggests that contribution of this bond in the π-electron conjugation is negligible.

4.3. CH_2Cl rotation barriers

To obtain the CH_2Cl rotational barriers, we have varied the ClCCO dihedral angle (Φ) in MCACP from −80 to 280° in steps of 10° separately for both groups and calculated the potential energies at the B3LYP/6-311++G(d,p) level by fixing all other structural parameters at their optimized equilibrium positions. The calculated potential energy curves as function of Φ are shown in Fig. 5.

Rotation of the CH_2Cl group about C6—C12 bond generates two barrier energies (see Fig. 5, curve a). During this rotation the torsion angle of the second CH_2Cl group is constantly near −99°, which is the optimized value for this dihedral angle. The first barrier to rotation occurs at 6° (ΔE = 17.6 kJ/mol) and the second barrier obtained at 176° (ΔE = 188.2 kJ/mol).

Fig. 5 curve b shows that the rotation of CH_2Cl group connected to C8 also creates two barriers (one at a torsion angle of 26° with a barrier of 10.0 kJ/mol and the other at a torsion angle of 196° with a barrier of about 204.6 kJ/mol). In this case, the torsion angle of the other CH_2Cl group is constantly near −84°.

In the third case both CH_2Cl groups were rotated simultaneously in opposite directions. As it is shown in Fig. 5 curve c, this rotation generates two high barrier energies. One barrier (ΔE = 221.8 kJ/mol) is related to the repulsive interaction between Cl20 and O7 atoms, whilst the other barrier (ΔE = 196.6 kJ/mol) is caused by repulsive interaction between Cl21 and O9 atoms.

By this method, we only obtained two stable chelated conformers (A-I and A-II) which are shown in Fig. 2. According to Fig. 5, the barrier for conversion of both stable enol conformers is 17.6 kJ/mol

Table 1
Selected bond distances (Å) and bond angles (°) of calculated stable chelate and open MCACP conformers and fulvene at B3LYP/6-311++G(d,p) level.[a]

	A-I		A-II		B-I		B-II		Fulvene
	G	S	G	S	G	S	G	S	G
Bond distances									
C1—C2	1.474	1.476	1.474	1.476	1.474	1.473	1.472	1.474	1.474
C1—C5	1.434	1.434	1.434	1.434	1.458	1.457	1.459	1.456	1.474
C2—C3	1.397	1.399	1.397	1.399	1.379	1.380	1.377	1.382	1.351
C4—C5	1.382	1.382	1.382	1.382	1.365	1.364	1.364	1.366	1.351
C3—C4	1.416	1.415	1.416	1.415	1.438	1.439	1.439	1.435	1.475
C1—C6	1.387	1.386	1.387	1.387	1.368	1.369	1.367	1.370	1.341
C2—C8	1.431	1.428	1.431	1.428	1.468	1.470	1.468	1.462	–
C6—O7	1.302	1.304	1.303	1.303	1.330	1.332	1.331	1.331	–
C8—O9	1.249	1.251	1.249	1.251	1.217	1.215	1.217	1.221	–
C6—C12	1.504	1.502	1.504	1.502	1.503	1.497	1.503	1.498	–
C8—C11	1.521	1.520	1.522	1.520	1.536	1.534	1.534	1.534	–
O7—H10	1.035	1.035	1.035	1.036	0.969	0.967	0.969	0.967	–
H10···O9	1.462	1.458	1.464	1.455	–	–	–	–	–
O7···O9	2.489	2.487	2.490	2.484	2.742	2.807	2.762	2.775	–
C4—H14	1.080	1.080	1.080	1.080	1.080	1.080	1.081	1.080	1.081
C5—H13	1.080	1.080	1.080	1.080	1.081	1.080	1.080	1.080	1.081
C3—H15	1.081	1.080	1.081	1.080	1.081	1.081	1.081	1.081	1.081
C12—H18	1.087	1.087	1.087	1.087	1.091	1.090	1.091	1.090	–
C12—Cl20	1.819	1.828	1.819	1.828	1.826	1.834	1.826	1.834	–
C11—Cl21	1.817	1.826	1.816	1.826	1.821	1.808	1.817	1.827	–
C11—H16	1.086	1.086	1.086	1.086	1.086	1.086	1.086	1.086	–
Bond angles									
O7—H10···O9	170.7	171.6	170.4	171.6	–	–	–	–	–
C2C1C5	106.1	106.1	106.1	106.1	106.1	106.2	106.2	106.1	106.1
C1C2C3	106.6	106.5	106.6	106.5	106.6	106.6	106.7	106.5	107.9
C3C4C5	108.5	108.6	108.5	108.6	108.5	108.6	108.5	108.5	109.0
C2C1C6	129.2	129.1	129.2	129.0	129.8	129.3	129.3	130.0	126.9
C1C2C8	127.9	127.9	127.9	127.9	128.6	128.0	128.4	128.9	–
C1C6O7	125.1	125.0	125.1	125.0	121.8	120.8	121.6	121.2	–
C2C8O9	124.0	124.2	124.0	124.2	124.4	124.1	124.0	124.6	–
C6O7H10	110.8	110.5	110.9	110.5	110.3	111.4	110.3	111.3	–
C1C5H13	125.6	125.7	125.6	125.7	126.0	125.7	126.0	125.7	124.5
C5C4H14	126.0	126.0	126.0	126.0	126.2	126.3	126.2	126.3	126.5
C2C3H15	125.6	125.8	125.6	125.8	125.5	126.0	125.7	125.8	126.5
Φ1	−84.2	−77.5	83.8	77.6	−44.4	−45.9	43.3	63.1	–
Φ2	−98.8	−88.8	−98.6	−85.9	−122.1	−112.7	−122.8	−110.9	–

[a] Φ1 and Φ2 stand O7C6C12Cl20 and O9C8C11Cl21 dihedral angels, respectively; G and S stand for calculations in the gas phase and in acetone solution, respectively.

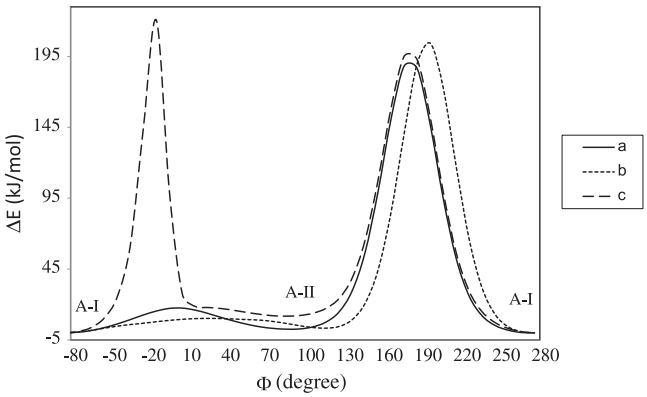

Fig. 5. The calculated potential surface of the CH_2Cl groups torsion as function of ClCCO dihedral angle (Φ). (a) Rotation about C6—C12 bond; (b) rotation about C8—C11 bond; (c) simultaneous and opposite rotation of both CH_2Cl groups.

Table 2
Relative energy (E_R), E_{HB}, and dipole moments (μ) for MCACP conformers obtained at the B3LYP level using various basis sets and different media.

Basis sets	E_R (kJ/mol)		E_{HB} (kJ/mol)	
	A-I	A-II	A-I	A-II
6-31G(d,p)[d]	0.00	0.67	85.90	82.38
6-311G(d,p)[d]	0.00	0.71	83.39	79.54
6-311++G(d,p)[d]	0.00	0.63	76.94	74.35
6-311G(d,p)[a]	0.00	0.50	71.04	71.13
6-311G(d,p)[b]	0.00	0.17	67.86	66.78
6-311++G(d,p)[a]	0.00	0.46	65.81	65.10
6-311++G(d,p)[c]	0.00	0.08	61.88	61.84
MP2/6-31G(d,p)[d]	0.00	0.63	72.97	72.13
μ [b](Debye)	4.0	5.9		
μ [d](Debye)	2.5	4.0		

[a] Calculated in chloroform.
[b] Calculated in acetone.
[c] Calculated in DMSO.
[d] Calculated in the gas phase.

and their energy difference is only 0.63 kJ/mol in the gas phase and 0.46 kJ/mol in the chloroform solution (see Table 2). Therefore, it is likely that both enol conformers to be coexisted in the sample. Unfortunately, because of similarity in their vibrational spectra and rapid conversion of these two enol conformers in the NMR time scale, it was not possible to distinguish the existing of both conformers in the sample.

4.4. Hydrogen bond strength

The calculated relative and hydrogen bond energies (obtained at the B3LYP level using 6-311++G(d,p), 6-311G(d,p), and 6-31G(d,p) basis sets) along with the dipole moments are collected in Table 2. Table 3 compares the Gilli's internal coordinates (q_1, q_2, Q) [42], and the calculated OH stretching, in-plane bending, and out-of-plane bending vibrational wavenumbers for A-I and A-II conformers. For comparison, the corresponding parameters for AA [38], benzoylacetone (BA) [43], MA [37,44], and nitromalonaldehyde (NO_2MA) [37] are also given in Table 3. The calculated A-I hydrogen bond energy, E_{HB}, (the energy difference between the chelated and its corresponding open form) in the gas phase and in the chloroform and acetone solutions is 83.4, 71.0, 67.9 kJ/mol, respectively. The results show that the hydrogen bond strength decreases in solution. The calculated E_{HB} of A-I is higher than the corresponding value for A-II in both gas phase and solution.

The effect of the CP ring on the π-electron delocalization in the chelated ring could also be explained in the terms of the Gilli's symmetry coordinates [42] q_1 (dC—O-dC=O), q_2 (dC—C-dC=C), and Q ($Q = q_1 + q_2$), (see Table 3). Bertolasi et al. [42] showed that the values of $q_1 = 0.15$ and $q_2 = 0.17$ for the standard bond distances in the absence of π-delocalization lead to $Q = 0.32$ for the completely π-localized enol forms, while $Q = 0.0$ corresponds to the fully π-delocalized structures [42]. Table 3 indicates that q_1, q_2, and Q values are equal in both enolic A-I and A-II conformations. As Table 3 indicates, the q_1, q_2, and Q values for MCACP are considerably less than that for β-diketones. It predicts that CP ring has a general role in development of π-electron delocalization and bond equalization in the chelated ring. As other parameters given in Table 3 indicate, the increase in the π-electron delocalization leads in much stronger hydrogen bond in MCACP than in β-diketones.

The comparison of bond orders of CP ring in MCACP (see Table 4) with that of fulvene molecule indicates more π-electron delocalization in the MCACP's CP ring than that in the fulvene molecule. Table 4 also shows that the C—C and C—O bond orders in MCACP are higher while the C=O (except for dibenzoylmethane (DBM) [45]) and C=C bond orders are lower than the corresponding values in AA, BA, and DBM [45], respectively. These results indicate that the π-electron delocalization in the C=C—O and C—C=O fragments of the chelated heptagonal ring of MCACP is highly increased.

The calculations predict a double-minimum low barrier potential function for this molecule that is consistent with the formation of a strong hydrogen bond system. This two dimensional potential

Table 3
Comparing of parameters related to H-bond strength in MCACP with some β-diketones.[a]

	q_1(Å)	q_2(Å)	Q(Å)	RO···O (Å)	νOH (cm^{-1})	γOH (cm^{-1})	δOH (ppm)
A-I[b]	0.054	0.044	0.098	2.489	1697	1105	17.30
A-II[b]	0.054	0.044	0.098	2.490	1697	1105	17.30
B-I[b]	0.123	0.114	0.236	2.742	–	–	–
B-II[b]	0.114	0.101	0.215	2.762	–	–	–
A-I[c]	0.054	0.043	0.096	2.487	1697	1105	17.30
A-II[c]	0.053	0.042	0.096	2.484	1697	1105	17.30
AA[d]	0.074	0.080	0.154	2.544	−2800[g]	952[g]	15.40
BA[e]	0.074	0.070	0.144	2.496	2633	993	16.90
NO_2MA[f]	0.069	0.074	0.143	2.559	2880	911	13.75
MA[f]	0.081	0.074	0.155	2.587	2856[h]	873[h]	–

[a] Q, q1, and q2 are Gilli's symmetric parametrs which are explained in the text; νOH and γOH stand for OH stretching and out-of-plane bending vibrational frequencies, RO···O stands for O7···O9 distance; δOH stands for enol chemical shift.
[b] In the gas phase.
[c] In the chloroform solution.
[d] Data from Ref. [38].
[e] Data from Ref. [43].
[f] Data from Ref. [37].
[g] Data from Ref. [51].
[h] Data from Ref. [44].

Table 4
Comparison of bond orders of chelated ring of MCACP and β-diketones.

	C2—C8	C1=C6	C8=O9	C6—O7	O—H	C1—C2	C2—C3	C3—C4	C4—C5	C1—C5
A-I	1.2052	1.4097	1.5358	1.2375	0.5567	1.0942	1.4176	1.3199	1.5241	1.2253
A-II	1.2053	1.4097	1.5360	1.2373	0.5569	1.0941	1.4176	1.3199	1.5240	1.2253
Fulvene	–	1.7829	–	–	–	1.0779	1.7658	1.1106	1.7658	1.0779
AA[a]	1.1848	1.5522	1.5847	1.1598	0.6268					
4BA[a]	1.2003	1.5095	1.5673	1.1520	0.6144					
DBM[a]	1.2011	1.4998	1.5173	1.1594	0.6103					

[a] Data from Ref. [45].

Table 5
^{1}HNMR and ^{13}CNMR chemical shifts for diacylcyclopentadienes.[a]

1HNMR	Solvent	δOH (ppm)	δH (13,15)	δH (14)	δH (R)	Ref.
A-I[b]	Gas	17.18	7.52	6.61	4.36	T. W
A-II[b]	Gas	17.21	7.53	6.61	4.27	T. W
A-I[b]	$CDCl_3$	17.15	7.71	6.74	4.53	T. W
A-II[b]	$CDCl_3$	17.08	7.72	6.77	4.43	T. W
MCACP	$CDCl_3$	17.30	7.48	6.55	4.65	T. W
HFF	$CDCl_3$	16.10	7.17	6.37	8.57	[19]
DACP	$CDCl_3$	18.15	7.32	6.39	2.53	[19]
DCACP	$CDCl_3$	17.34	7.57	6.57	6.78	[23]
^{13}CNMR	Solvent	δC (6,8)	δC (1,2)	δC (3,5)	δC (4)	δC (R)
A-I[b]	Gas	188.89	130.89	146.08	129.29	52.02
A-II[b]	Gas	188.97	130.51	146.09	129.55	51.73
A-I[b]	$CDCl_3$	189.11	131.36	148.70	130.55	53.35
A-II[b]	$CDCl_3$	189.56	130.82	148.32	130.78	52.77
MCACP	$CDCl_3$	181.50	124.0	139.5	123.0	44.0
HFF	$CDCl_3$	176.00	126.5	141.2	125.2	-
DCACP	$CDCl_3$	176.88	120.92	140.27	126.72	66.27

[a] All theoretical calculations are obtained at the B3LYP/6-311++G(d,p) level; T.W, this work; R, CH_2Cl groups' C or H atoms.
[b] Calculated values.

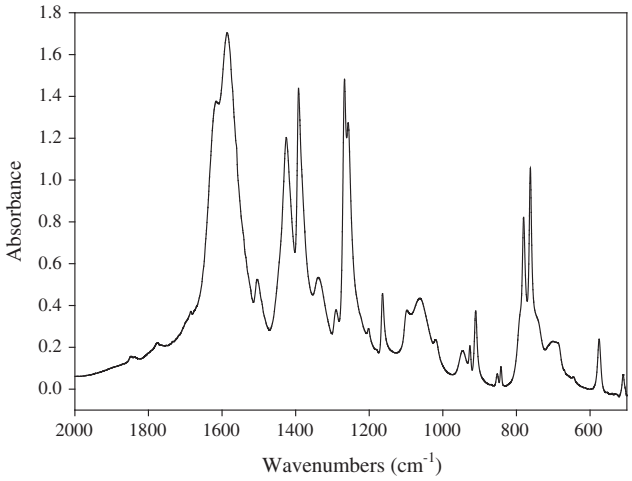

Fig. 6. Infrared spectrum of MCACP in the solid phase.

energy surface arises by coupling between the OH stretching and in-plane bending modes. The calculated barrier height for these results was about 11.7 kJ/mol. In addition, the calculated tunneling frequencies for MCACP and its deuterated analogue are about 480 and 170 cm^{-1}, respectively. The calculated barrier height at the B3LYP/6-311++G(d,p) level for HFF [46], the simplest member of the diacylcyclopentadiene compounds, was estimated to be in the 16.5–17.9 kJ/mol range and its corresponding tunneling frequencies was predicted to be in the 296–330 cm^{-1} range for different energy cutoffs [46]. The calculated barrier height for MA [47] is

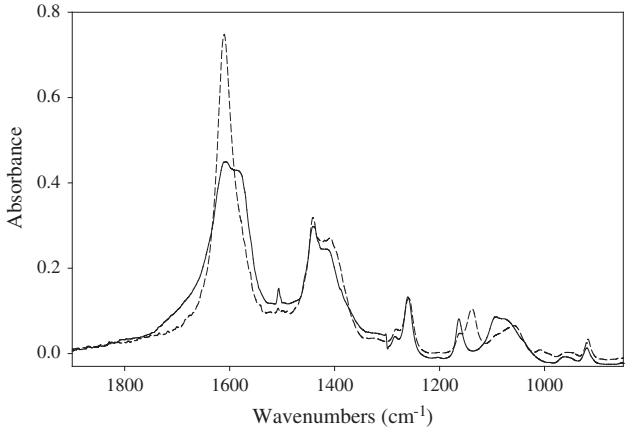

Fig. 7. Comparing the IR spectra of MCACP (—) and D-MCACP (- - -) in the CCl_4 solution (850–1900 cm^{-1} range).

49.3–53.6 kJ/mol, which is considerably higher than the corresponding value obtained for HFF and MCACP. Comparing these results reveals that the proton transfer between two oxygen atoms in MCACP is easier than that of HFF and MA. According to Table 1 the hydrogen bond angle in MCACP is close to the linear system ($\theta_{O—H\cdots O}$ = 170.5°) while the O—H···O system in MA considerably deviates from linearity, ($\theta_{O—H\cdots O}$ = 145.9–148.6°) [46]. These results describe the lower barrier height for proton tunneling in MCACP than that in MA.

4.5. NMR analysis

Table 5 shows the experimental and calculated ^{1}HNMR and ^{13}CNMR chemical shifts for both stable conformers of MCACP. The NMR spectra were recorded in dilute solutions of $CDCl_3$ and the calculated chemical shifts obtained by using GAIO method. In this method the isotropic shieldings (σ) are commonly compared with experiment and similar compounds. Proton isotropic shieldings are practically sensitive to the basis set size and quality. However, the corresponding chemical shift values are less sensitive to the basis set and method of calculation. The basis set 6-311G(d,p) gives fairly accurate NMR spectral data. Significantly better results are obtained using the larger basis set (6-311++G(d,p)).

Solvent effects, assuming solvent is considered chloroform, for MCACP are included using the PCM (calculated at the B3LYP/6-311++G(d,p) level). According to these results, the calculated chemical shifts are in good agreement with the experimental findings.

Table 5 indicates that the chemical shift for the enolic proton of MCACP (17.30 ppm) occurs at higher frequency (less shielding) than that for HFF (16.10 ppm) while is lower than that for DACP (18.15 ppm). These results could be described by considering both steric and electron withdrawing effects of CH_2Cl groups simultaneously.

4.6. Interpretation of IR spectrum

The fundamental vibrational frequencies of both stable enol conformations and their deuterated analogous are calculated at the B3LYP/6-311++G (d,p) basis set, for the gas phase and solution. The theoretical frequencies were assigned and compared with the experimental data. The results indicate that the calculated frequencies are slightly higher than the observed values for the majority of the normal modes. The difference between the computed and experimental frequencies may be due to many different factors that are usually not even considered in the theory, such as anharmonicity, Fermi resonance, and solvent effects. Scaling of the theoretical wavenumbers according to the equation $\nu_{Exp.} = \alpha\nu Calc.$ generally leads to satisfactory agreement with the set of observed wavenumbers. In this work, we used 0.9609 and 0.9859 scaling factors for high and low frequencies, respectively, which is suggested by Tayyari et al. [48]. The IR spectrum of MCACP in the solid phase is illustrated in Fig. 6. Fig. 7 compares the IR spectra of

Table 6
Theoretical and experimental vibrational frequencies (cm^{-1}) of MCACP.[a]

Theoretical										Experimental		Assignments
$F_{A\text{-}I}$	I_{IR}	A_R	$F_{A\text{-}II}$	I_{IR}	A_R	F_{A-I}^{*}	I_{IR}	F_{A-II}^{*}	I_{IR}	IR_{Solid}	IR_{CCl4}	
3112	3	195	3112	3	194	3113	4	3113	4	3112(sh)	3108(sh)	1
3100	3	60	3100	3	61	3102	3	3101	3	3100(w)	3095(w)	2
3090	1	71	3090	2	71	3091	2	3091	2	3090(w)	3088(sh)	3
3065	0	29	3065	1	30	3073	1	3074	1	3079(vw)	3080(sh)	$\nu as CH_2$
3055	0	46	3054	1	48	3062	1	3060	1	3043(vw)	3055(vw)	$\nu as CH_2$
2997	5	126	2996	6	132	3000	5	3000	5	2985(w)	2993(w)	νsCH_2
2990	7	106	2989	7	108	2997	7	2995	7	2985(w)	2986(sh)	νsCH_2
2363	939	65	2371	930	67	2362	1204	2358	1205	1697(w)	1690(w)	νOH
1635	690	88	1633	711	89	1626	824	1625	830	1616(sh)	1610(sh)	δOH,νC=C
1592	203	61	1591	179	64	1582	450	1581	441	1587(s)	1574(m)	δOH,νC=O
1530	36	19	1530	36	18	1528	59	1527	60	1528(vw)	–	4,νsC—C=O,νC—O
1505	13	19	1503	17	17	1504	15	1503	17	1504(w)	1506(w)	5,δOH
1467	63	5	1467	61	8	1463	94	1465	87	1455(sh)	1457(vw)	CH_2 sci
1458	14	14	1457	17	8	1457	10	1457	19	1441(sh)	1441(m)	CH_2 sci
1432	102	57	1432	100	58	1429	145	1429	142	1425(m)	1411(m)	6, νC—C, νC—O
1402	69	20	1402	79	16	1400	78	1400	84	1393(s)	1390(sh)	7, νC—C,νC—O
1385	175	76	1384	166	77	1383	248	1383	246	1384(sh)	1383(w)	8, νC=C
1320	74	179	1319	75	188	1314	127	1313	129	1319(w)	–	9, νC—C, ωCH_2
1287	1	19	1286	1	20	1285	3	1284	2	1285(sh)	1285(vw)	10, ωCH_2
1278	11	40	1278	30	28	1276	16	1276	41	1269(s)	1270(sh)	ωCH_2
1274	29	5	1274	7	10	1272	40	1271	10	1267(s)	1260(w)	ωCH_2
1210	3	5	1210	3	5	1211	4	1210	3	1201(w)	–	11
1174	60	15	1173	62	16	1171	85	1171	82	1163(w)	1163(w)	τCH_2
1159	5	9	1159	2	5	1157	3	1156	4	1159(sh)	–	τCH_2
1122	96	1	1116	88	16	1110	42	1111	56	1105(sh)	1105(sh)	γOH
1109	25	59	1109	30	44	1107	113	1106	99	1097(w)	1096(w)	13, τCH_2
1063	72	8	1062	73	7	1060	96	1059	95	1061(w)	1065(sh)	14, τCH_2
1041	11	27	1039	12	22	1038	16	1038	17	–	1040(sh)	15, ρCH_2
969	12	5	969	12	6	967	18	967	18	946(vw)	965(vw)	16, ρCH_2
927	4	4	928	5	2	929	1	928	4	928(w)	920(w)	ρCH_2
926	1	0	923	1	1	925	7	926	5	926(w)	918(w)	17, ρCH_2
918	12	4	918	12	5	916	19	916	17	910(w)	910(sh)	ρCH_2,17
870	2	3	869	2	4	873	2	873	2	–	–	18
841	1	17	840	1	16	839	1	839	2	840(vw)	840(vw)	19
779	1	18	779	1	8	779	2	778	2	779(m)	–	20, νCCl
774	0	7	773	38	22	773	51	772	48	774(sh)	–	νCCl, 22
746	41	15	745	19	18	746	19	746	22	740(w)	–	23, νCCl
697	17	30	696	101	12	690	43	690	126	684(31)	–	δR-C=O, δR-C—O
677	29	14	680	25	17	671	227	676	41	676(sh)	–	24, δR-C=O, δR-C—O
656	168	31	651	65	6	658	1	651	91	644(vw)	–	25
586	29	3	603	30	65	584	37	601	43	–	–	26, γR-C=O
573	1	0	574	4	0	571	4	573	5	574(w)	–	27
573	5	40	553	1	7	570	6	552	2	574(w)	–	26, νCCl
515	1	12	517	1	11	514	1	517	1	510(w)	–	νOH···O, δC—C=O, δCCl
501	2	2	501	3	3	501	4	501	4	499(sh)	–	δC5C1C6, δC1C2C3
393	1	4	392	1	4	393	0	392	1	390(vw)	–	δC1C2C7, δC2C1C6
367	4	4	367	5	3	364	5	363	6	366(sh)	–	νOH···O, δC—C-R, δCCl
275	10	1	277	9	2	276	13	278	12	270(vw)	–	δC—C-R
248	8	3	248	8	3	252	11	252	11	–	–	δC—C-R
229	2	0	224	1	0	231	3	227	1	–	–	29
205	1	2	211	2	1	203	2	212	2	–	–	ρR
173	0	0	158	0	1	175	1	159	1	–	–	γC—O, γC=O, 29
140	0	2	141	0	2	138	0	142	0	–	–	γC—O, γC=O, 28
87	0	4	95	2	3	85	0	94	3	–	–	πC-R
44	2	6	46	1	3	39	3	40	1	–	–	τR
40	1	0	36	1	4	38	0	36	2	–	–	γR
29	2	0	32	0	2	28	3	30	0	–	–	τR

[a] F stands for scaled (by 0.9609 and 0.9859 for higher and lower than 1700 cm^{-1}) wavenumbers calculated at the B3LYP/6-311++G(d,p) I_{IR}, infrared intensity in KM/mol; A_R, Raman scattering activities in A4/amu; R, CHCl2 group; ν, stretching, δ, in-plane bending; γ, out-of-plane bending, ρ, in-plane rocking; π, out-of-plane bending mode; ω, wagging; τ, torsion; s, strong; m, medium; w, weak; vw, very weak; sh, shoulder.

* Calculated in CCl_4 solution.

MCACP and its deuterated analogous in solution. The scaled vibrational band frequencies and their assignments for the enol form of MCACP and its corresponding deuterated analogous along with the observed infrared frequencies are listed in Tables 6 and 7, respectively. According to these tables, the calculated wavenumbers obtained in solution and gas phase, except for a few cases, are almost the same. Deconvoluted IR spectrum of MCACP in the 1750–1300 cm^{-1} region is shown in Fig. 8.

The notations for cyclopentadienyl group vibrations are according to the normal modes of CP ring, which have been recently reported for DCACP molecule [23].

4.6.1. 3500–1700 cm^{-1} region

In this region the OH and CH stretching frequencies are expected to be observed. The OH stretching band position is extremely related to the hydrogen bond strength. The enol form of β-diketones exhibits a broad band in the 3500–2200 cm^{-1} region, which upon deuteration of the enolic proton appears as a new narrower band in the 2200–1800 cm^{-1} region [37–39,45,47]. In systems with short (less than 2.50 Å for the O···O distance) and strong intramolecular hydrogen bonds, recognition of the OH-stretching peak is often debatable. Because of anharmonic effects, this vibrational mode is shifted to the lower-frequencies and may

Table 7
Theoretical and experimental vibrational frequencies (cm^{-1}) of D-MCACP.[a]

Theoretical										Experimental	Assignments
$F_{A\text{-}I}$	I_{IR}	A_R	$F_{A\text{-}II}$	I_{IR}	A_R	F_{A-I}^*	I_{IR}	F_{A-II}^*	I_{IR}	IR_{CCl4}	
3112	3	195	3112	3	194	3113	4	3113	4	3108(sh)	1
3100	3	60	3100	3	61	3102	4	3101	4	3095(w)	2
3090	2	71	3090	2	71	3091	2	3091	2	3088(sh)	3
3066	1	29	3065	1	30	3073	1	3074	1	3080(sh)	$\nu asCH_2$
3054	1	47	3054	1	49	3062	1	3060	1	3055(vw)	$\nu asCH_2$
2997	5	126	2996	5	131	3000	5	3000	5	2996(w)	νsCH_2
2989	7	106	2989	7	108	2997	7	2995	7	2980(sh)	νsCH_2
1792	656	7	1793	653	7	1783	853	1781	853	–	νOD
1616	788	66	1616	787	67	1603	1108	1603	1106	1609(s)	νC═C—O, νC═O
1534	60	63	1534	60	64	1531	106	1530	107	–	νC═O, C—C,4
1517	10	37	1517	8	35	1515	24	1514	27	1508(vw)	5, νC═O, νOD
1468	74	6	1468	73	8	1463	100	1466	97	1441(m)	CH_2 sci
1457	8	14	1457	10	8	1457	5	1456	12	–	CH_2 sci
1430	72	62	1430	70	61	1428	106	1428	103	1407(m)	6, νC—O, CH_2 sci
1412	1	39	1412	2	35	1410	2	1411	4	1388(sh)	νC—C, 6, CH_2 sci
1389	211	58	1389	212	60	1387	279	1387	279	1364(sh)	8, νC═C, O-D
1318	67	190	1318	68	201	1312	113	1311	115	–	9, νC—C, ωCH_2
1286	1	20	1286	1	22	1285	4	1284	3	1282(vw)	10, ωCH_2
1278	8	40	1278	25	28	1276	13	1276	35	1260(w)	ωCH_2
1274	26	7	1274	8	11	1272	36	1271	10	1246(sh)	ωCH_2
1219	4	6	1218	4	6	1219	7	1219	6	–	11, δOD, τCH_2
1194	4	26	1193	4	25	1193	4	1192	4	1163(w)	12, δOD, τCH_2
1159	8	6	1159	4	4	1157	8	1157	6	–	τCH_2
1149	88	2	1149	93	4	1147	130	1146	130	1137(w)	τCH_2, δOD, 13
1100	7	37	1100	7	36	1100	10	1101	12	1080(sh)	13, δOD
1062	72	9	1061	72	9	1060	96	1058	93	1058(w)	14, τCH_2
1014	31	29	1012	32	24	1011	43	1011	45	1008(vw)	15, δOD, ρCH_2
966	8	9	966	7	11	964	11	964	11	966(vw)	16, ρCH_2
926	0	1	925	2	2	929	0	927	1	924(sh)	17, ρCH_2
924	3	3	922	1	2	923	4	923	4	918(w)	ρCH_2
917	12	3	918	12	5	915	20	916	18	909(sh)	ρCH_2
870	2	3	869	2	4	873	2	873	2	847(vw)	18
840	1	16	840	1	16	839	1	839	2	823(vw)	19
817	63	0	814	59	1	807	72	807	66	–	γOD
779	1	20	779	1	8	778	1	778	2	–	20, νCCl
773	55	5	772	54	21	771	76	771	75	–	νCCl, 22, γOD
745	11	15	744	12	20	744	9	745	11	–	22, νCCl
696	34	28	675	15	15	689	49	672	26	–	νC1—C2, ρCH_2, νC—Cl
675	153	14	696	103	13	669	208	689	133	–	24, δR-C═O, νC—Cl
654	1	31	650	66	6	656	1	650	91	–	25, ρCH_2
584	26	3	600	27	64	583	33	598	38	–	26, γR-C═O
573	1	2	574	4	1	571	3	572	5	–	27
571	4	38	552	1	7	568	6	551	2	–	26, νCCl
504	2	9	504	2	11	503	4	504	2	–	δC═C—O, δC5C1C6
498	1	4	500	2	3	497	1	500	2	–	νOD···O, δC—C═O
390	0	3	389	0	3	390	0	389	0	–	δC1C2C7, δC2C1C6
364	4	4	364	5	3	361	6	360	7	–	νOH···O, δC—C-R, δCCl
274	10	1	277	9	2	276	13	278	12	–	δC—C-R
245	8	3	245	8	3	249	10	250	10	–	δC—C-R
229	2	1	224	1	0	230	3	226	1	–	29
204	1	2	211	2	1	203	2	211	2	–	ρR
172	1	0	157	0	1	174	1	157	1	–	γC—O, γC═O, 29
139	0	2	141	0	2	138	0	141	0	–	γC—O, γC═O, 28
87	0	4	95	2	3	85	0	94	3	–	πC-R
44	2	6	45	1	3	39	3	40	1	–	τR
40	1	0	36	1	4	38	0	36	2	–	γR
29	2	0	32	0	2	28	3	30	0	–	τR

[a] See footnotes of Table 6.

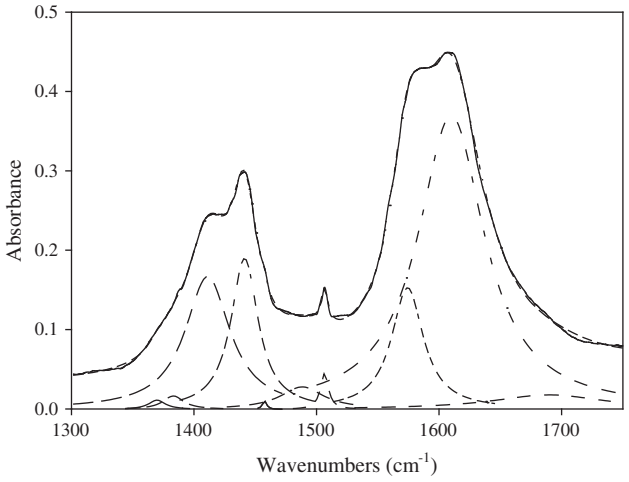

Fig. 8. Deconvoluted infrared spectrum of MCACP in the CCl_4 solution.

interact with other vibrational modes especially the OH in-plane bending (linked to the band near 1570 cm^{-1}). Such interaction was emphasized in the study by Stare and Balint-Kurti [49] and plays a crucial role in determining the appearance of the infrared spectrum. Similar effects were observed previously in studies of the hydrogen maleate ion [50]. Results show that the mixing of the OH stretch with other modes does not become important until the effective frequency for the OH-stretching normal mode drops below about 2200 cm^{-1} and that mixing becomes more significant the lower it becomes. According to the calculations, we expect to observe a very strong band in the IR spectrum of the title compound due to the OH stretching normal mode at about 2360 cm^{-1}. The corresponding band in DCACP is calculated at 2318 cm^{-1} [23]. This wavenumber shift indicates that the steric effect of Cl atoms in DCACP is compensated by their electron-withdrawing nature. Deconvolution of IR spectrum of MCACP indicates a broad and weak band at about 1690 cm^{-1}, which disappears upon deuteration. This band could be attributed to the OH stretching vibration. The corresponding band in the IR spectrum of DCACP was estimated at about 1720 cm^{-1} and 1690 cm^{-1} in the solution and solid phase, respectively [23].

Three relatively weak bands at 3108, 3095, and 3088 cm^{-1} in the IR spectrum of CCl_4 solution are assigned to the CH stretching vibrations of CP ring. In the CCl_4 solution IR spectrum of MCACP, four relatively weak bands were observed at 3080, 3055, 2993, and 2986 cm^{-1}. The first two bands are attributed to the asymmetric and the last two bands are assigned to the symmetric CH_2 stretching vibrations.

4.6.2. 1700–1000 cm^{-1} region

The strong band at 1610 cm^{-1} in the infrared spectrum of MCACP is related to the OH in-plane bending vibration which is strongly coupled to the C═C stretching vibration. According to our calculations, we expect to observe the OD in-plane bending band frequency at about 1200 cm^{-1}, which is strongly coupled to the CH in-plane bending of CP ring. In the solution this band is observed at 1163 cm^{-1}. The corresponding band in D-DCACP [23] was reported to be occurred at 1157 cm^{-1}, which is also coupled with one of the CP ring modes.

The strongest band in the IR spectrum of MCACP, which appears at 1587 cm^{-1}, is assigned to the OH in-plane bending vibration. This vibrational mode is strongly coupled to the C═O stretching movement. Beside these bands, the vibrational modes such as C—C and, C—O stretching and C—H bending are expected to be observed in this region. According to the theoretical calculations, two observed bands at 1425 and 1393 cm^{-1} in the solid state are assigned to the C—H bending of CP ring coupled with the C—C and C—O stretching movements. In the IR spectrum of MCACP in solution, these bands slightly show a blue shift and appear at 1411 and 1390 cm^{-1}, respectively.

The OH out-plane bending vibrational mode is observed at 1105 cm^{-1}, which is very close to that predicted by theoretical calculations (1122 cm^{-1}). Upon deuteration this band disappears. The corresponding band in DCACP occurs at 1074 cm^{-1} and 1088 cm^{-1} [23] in solution and in the solid phase, respectively. The OH out-plane bending vibration in the enol forms of β-diketones appears in the 900–980 cm^{-1} range [37,39,43,45], which is considerably lower than those observed for MCACP and DCACP compounds.

4.6.3. Below 1000 cm^{-1} region

In this region we expect to observe C—Cl stretching, C—CH_2Cl, CH out-of-plane bending, ring deformations, and torsional modes.

The two relatively weak bands at about 946 and 840 cm^{-1} in the IR spectrum of MCACP are assigned to the C═C—C in-of plane bending modes of CP ring.

The two medium bands at 779 and 740 cm^{-1} are assigned to the asymmetric and symmetric C—Cl stretching modes, respectively.

According to the calculated results, the 510 and 366 cm^{-1} bands are caused by mixing of O···O stretching skeletal vibrations. Therefore, it may be concluded that the O···O stretching frequency is higher than that in AA [51], trifluoro-acetylacetone (TFAA) [52], HFAA [39], and furoyl-trifluoroacetone (FTFA) [53], which is reported to be occurred at 366, 264, 240, and 319 cm^{-1}, respectively. These results also suggest much stronger hydrogen bond in MCACP than that in the enol form of β-diketones.

5. Conclusion

The rotation of the CH_2Cl groups about C6—C12 and C8—C11 indicates that the enolic structure of MCACP has two conformers that are stabilized by formation of an intramolecular hydrogen bond. The calculated results show that the stabilities of these chelated enol conformers are very close to each other. The energies of these enol forms are considerably lower (about 54–71 kJ/mol) than those of the possible keto forms. This high stability of the enol forms is due to the formation of short and strong intramolecular hydrogen bond. Moreover, the NICS results indicate that aromaticity increase of CP ring is mainly caused by intramolecular hydrogen bond formation. The high energy difference between keto and enol tautomers suggests that the presence of keto forms in the MCACP sample is unlikely and MCACP predominantly exists in the enol form.

The theoretical calculations and experimental data support the formation of a short and very strong intramolecular hydrogen bond in MCACP molecule.

Comparing the theoretical and experimental results for MCACP with the corresponding values in the enol forms of β-diketones indicate that the intramolecular hydrogen bond in MCACP is much stronger than that in the enol forms of β-diketones.

Appendix A. Supplementary material

Supplementary data associated with this article can be found, in the online version, at http://dx.doi.org/10.1016/j.molstruc.2013.01.031.

References

[1] C.C. Chen, S.F. Shyu, Int. J. Quantum Chem. 76 (2000) 541–551.
[2] R.S. Haddon, J. Am. Chem. Soc. 102 (1980) 1807–1811.
[3] J. Higgins, Z. Zhou, L. Liu, T.T.S. Huang, J. Phys. Chem. A 101 (1997) 2702–2708.

[4] N.I. Giricheva, G.V. Girichev, S.B. Lapshina, N.I. Kuzmina, J. Struct. Chem. 41 (2000) 48–54.
[5] V.B. Delchev, H. Mikosch, G.S. Nikolov, Monatshefte fur Chemie 132 (2001) 339–348.
[6] M. Huang, J. Zou, D. Yang, B. Ning, Zh. Shang, Q. Yu, J. Mol. Struct. (Theochem) 589 (2002) 321–328.
[7] V.B. Delchev, G.S. Nikolov, Monatshefte fur Chemie 131 (2000) 99–105.
[8] S.F. Tayyari, A. Najafi, F. Lorestani, R.E. Sammelson, J. Mol. Struct. (Theochem) 854 (2008) 54–62.
[9] G. Gilli, F. Bellucci, V. Ferretti, V. Bertolasi, J. Am. Chem. Soc. 111 (1989) 1023–1028.
[10] J.A. Gerlt, P.G. Gassman, J. Am. Chem. Soc. 114 (1992) 5928–5934.
[11] J.A. Gerlt, P.G. Gassman, J. Am. Chem. Soc. 115 (1993) 11552–11568.
[12] J.A. Gerlt, P.G. Gassman, Biochemistry 32 (1993) 11943–11952.
[13] W.W. Cleland, P.A. Frey, J.A. Gerlt, J. Biol. Chem. 273 (1998) 25529–25532.
[14] W.W. Cleland, M.M. Kreevoy, Science 264 (1994) 1887–1890.
[15] K.S. Kim, D. Kim, J.Y. Lee, P. Tarakeshwar, K.S. Oh, Biochemistry 41 (2002) 5300–5306.
[16] J. Abildgaard, S. Bolvig, P.E. Hansen, J. Am. Chem. Soc. 120 (1998) 9063–9069.
[17] P.E. Hansen, S. Bolvig, K. Wozniak, J. Mol. Struct. 749 (2005) 155–168.
[18] H. Fuess, H.J. Lindner, Chem. Ber. 108 (1975) 3096–3104.
[19] M. Rajabi, M.Sc. thesis, University of Ferdowsi, Mashhad, Iran, 1994.
[20] D. Lloyd, N.W. Preston, J. Chem. Soc. C (1969) 2464–2469.
[21] G. Gilli, V. Bertolasi, The chemistry of enols, in: Z. Rappoport (Ed.), John Wiley and Sons, N.Y., 1990.
[22] M.H. Arbab Zavar, S.F. Tayyari, S. Evazmoghadam, M. Chamsaz, Asian J. Chem. 19 (2007) 271–282.
[23] S.F. Tayyari, S. Laleh, M. Zahedi-Tabrizi, M. Vakili, J. Mol. Struct. 1036 (2013) 151–160.
[24] Gaussian 09, Revision A.02, M.J. Frisch, G.W. Trucks, H.B. Schlegel, G.E. Scuseria M.A. Robb, J.R. Cheeseman, G. Scalmani, V. Barone, B. Mennucci, G.A. Petersson, H. Nakatsuji, M. Caricato, X. Li, H.P. Hratchian, A.F. Izmaylov, J. Bloino, G. Zheng, J.L. Sonnenberg, M. Hada, M. Ehara, K. Toyota, R. Fukuda, J. Hasegawa, M. Ishida, T. Nakajima, Y. Honda, O. Kitao, H. Nakai, T. Vreven, J.A. Montgomery, Jr., J.E. Peralta, F. Ogliaro, M. Bearpark, J.J. Heyd, E. Brothers, K.N. Kudin, V.N. Staroverov, R. Kobayashi, J. Normand, K. Raghavachari, A. Rendell, J.C. Burant, S.S. Iyengar, J. Tomasi, M. Cossi, N. Rega, J.M. Millam, M. Klene, J.E. Knox, J.B. Cross, V. Bakken, C. Adamo, J. Jaramillo, R. Gomperts, R.E. Stratmann, O. Yazyev, A.J. Austin, R. Cammi, C. Pomelli, J.W. Ochterski, R.L. Martin, K. Morokuma, V.G. Zakrzewski, G.A. Voth, P. Salvador, J.J. Dannenberg, S. Dapprich, A.D. Daniels, O. Farkas, J.B. Foresman, J.V. Ortiz, J. Cioslowski, D.J. Fox, Gaussian, Inc., Wallingford CT, 2009.
[25] A.D. Becke, J. Chem. Phys. 98 (1993) 5648–5652.
[26] C. Lee, W. Yang, R.G. Parr, Phys. Rev. B 37 (1988) 785–789.
[27] GaussView 5.0.8, Gaussian Inc., Garnegie Office, Park, Pittsburgh, PA 15106, USA.
[28] S. Miertus, E. Scrocco, J. Tomasi, Chem. Phys. 55 (1981) 117–129.
[29] S. Miertus, J. Tomasi, Chem. Phys. 65 (1982) 239–245.
[30] M. Cossi, V. Barone, R. Cammi, J. Tomasi, Chem. Phys. Lett. 255 (1996) 327–335.
[31] J.R. Cheeseman, G.W. Trucks, T.A. Keith, M.J. Frisch, J. Chem. Phys. 104 (1996) 5497–5509.
[32] K. Wolinski, J.F. Hilton, P. Pulay, J. Am. Chem. Soc. 112 (1990) 8251–8260.
[33] P.v.R. Schleyer, Ch. Maerker, A. Dransfeld, H. Jiao, N.J.R. van Eikema Hommes, J. Am. Chem. Soc. 118 (1996) 6317–6318.
[34] E.D. Glendening, J.K. Badenhoop, A.E. Reed, J.E. Carpenter, J.A. Bohmann, C.M. Morales, F. Weinhold NBO 5.0.
[35] Genplot Package Computer Graphic Service, Cornel University, Utica, New York, 1990.
[36] W.J. Linn, W.H. Sharkey, J. Am. Chem. Soc. 79 (1957) 4970–4972.
[37] S.F. Tayyari, Z. Moosavi-Tekyeh, M. Zahedi-Tabrizi, H. Eshghi, J.S. Emampour, H. Rahemi, M. Hassanpour, J. Mol. Struct. 782 (2006) 191–199.
[38] S.F. Tayyari, F. Naghavi, S. Pojhan, R.W. McClurg, R.E. Sammelson, J. Mol. Struct. 987 (2011) 241–254.
[39] S.F. Tayyari, F. Milani-Nejad, H. Rahemi, Spectrochim. Acta, Part A 58 (2002) 1669–1679.
[40] G. Ferguson, W.C. Marsh, R.J. Restivo, D. Lloyd, J. Chem. Soc. Perkin Trans. 2 (1975) 998–1004.
[41] S.F. Tayyari, J.S. Emampour, M. Vakili, A.R. Nekoei, H. Eshghi, S. Salemi, M. Hassanpour, J. Mol. Struct. 794 (2006) 204–214.
[42] V. Bertolasi, P. Gilli, V. Ferretti, G. Gilli, J. Am. Chem. Soc. 113 (1991) 4917–4925.
[43] S.F. Tayyari, B. Chahkandi, J. Mol. Struct. 1015 (2012) 74–85.
[44] S.F. Tayyari, F. Milani-Nejad, Spectrochim. Acta, Part A 54 (1998) 255–263.
[45] S.F. Tayyari, H. Rahemi, A.R. Nekoei, M. Zahedi-Tabrizi, Y.A. Wang, Spectrochim. Acta, Part A 66 (2007) 394–404.
[46] S.F. Tayyari, M. Zahedi-Tabrizi, H. Rahemi, H.A. Mirshahi, J.S. Emampour, M. Rajabi, F. Milani-Nejad, J. Mol. Struct. (Theochem) 730 (2005) 17–21.
[47] S.F. Tayyari, M. Zahedi-Tabrizi, F. Tayyari, F. Milani-Nejad, J. Mol. Struct. (Theochem) 637 (2003) 171–181.
[48] S.F. Tayyari, T. Bakhshi, S.J. Mahdizadeh, S. Mehrani, R.E. Sammelson, J. Mol. Struct. 938 (2009) 76–81.
[49] J. Stare, G.G. Balint-Kurti, J. Phys. Chem. A 107 (2003) 7204–7214.
[50] F. Avberlj, M. Hodoscek, D. Hadzi, Spectrochim. Acta, Part A 41 (1985) 89–97.
[51] S.F. Tayyari, F. Milani-Nejad, Spectrochim. Acta, Part A 56 (2000) 2679–2691.
[52] M. Zahedi-Tabrizi, F. Tayyari, Z. Moosavi-Tekyeh, A. Jalali, S.F. Tayyari, Spectrochim. Acta, Part A 65 (2006) 387–396.
[53] S.F. Tayyari, A.R. Nekoei, H. Rahemi, J. Mol. Struct. 882 (2008) 153–167.